Published in final edited form as:
Neuroimage. 2014 November 15; 102(0 2): 828–837. doi:10.1016/j.neuroimage.2014.08.059.

Alterations of Hippocampal Projections in Adult Macaques with Neonatal Hippocampal Lesions: A Diffusion Tensor Imaging Study

Yuguang Meng[1], **Christa Payne**[2], **Longchuan Li**[3], **Xiaoping Hu**[3], **Xiaodong Zhang**[1,4,*], and **Jocelyne Bachevalier**[2,*]

[1]Yerkes Imaging Center, Yerkes National Primate Research Center, Emory University, Atlanta, Georgia, United States

[2]Yerkes National Primate Research Center and Department of Psychology, Emory University, Atlanta, Georgia, United States

[3]Marcus Autism Center, Children's Healthcare of Atlanta, Emory University, Atlanta, Georgia, United States

[4]Division of Neuropharmacology and Neurologic Disease, Yerkes National Primate Research Center, Emory University, Atlanta, Georgia, United States

Abstract

Neuropsychological and brain imaging studies have demonstrated persistent deficits in memory functions and structural changes after neonatal neurotoxic hippocampal lesion in monkeys. However, the relevant microstructural changes in the white matter of affected brain regions following this early insult remain unknown. This study assessed white matter integrity in the main hippocampal projections of adult macaque monkeys with neonatal hippocampal lesions, by diffusion tensor imaging (DTI). Data analysis was performed using tract-based spatial statistics (TBSS) and compared with volume of interest statistics. Alterations of fractional anisotropy (FA) and diffusivity indices were observed in fornix, temporal stem, ventromedial prefrontal cortex and optical radiations. To further validate the lesion effects on the prefrontal cortex, probabilistic diffusion tractography was used to examine the integrity of the fiber connections between hippocampus and ventromedial prefrontal cortex, and alterations were found in these connections. In addition, increased radial diffusivity in the left ventromedial prefrontal cortex correlated negatively with the severity of deficits in working memory in the same monkeys. The findings revealed microstructural changes due to neonatal hippocampal lesion, and confirmed that neonatal neurotoxic hippocampal lesions resulted in significant and enduring functional alterations in the hippocampal projection system.

*Correspondence to: Dr. Xiaodong Zhang, 954 Gatewood Rd NE, Atlanta, GA 30329, USA, Telephone: 1-404-712-9874, Fax: 1-404-712-9917, xzhang8@emory.edu, Dr. Jocelyne Bachevalier, 954 Gatewood Rd NE, Atlanta, GA 30329, USA, Telephone: 404-727-9765, Fax: 404-727-8088, jbachev@emory.edu.

Keywords

fornix; ventromedial prefrontal cortex; temporal stem; white matter integrity

Introduction

The hippocampus exhibits a pronounced vulnerability to hypoxic, ischemic or metabolic noxious events and behavioral stress, and is highly susceptible to epileptogenic mechanisms that have been associated with a spectrum of neurological diseases and psychiatric disorders (Bartsch, 2012). For example, children and adolescents that had suffered hypoxia-ischemia perinatally or later in childhood due to cardiac, respiratory, or other neurological disorders or their treatments have been diagnosed with severe long-term memory impairment (Adlam et al., 2009; de Haan et al., 2006; Gadian et al., 2000; Vargha-Khadem et al., 1997). Memory impairment in these cases has been mainly ascribed to selective bilateral hippocampal atrophy (Bachevalier and Vargha-Khadem, 2005). However, alterations of other brain structures, such as posterior thalamus, putamen, and retrosplenial cortex are also present in these cases (Vargha-Khadem et al., 2003) and could likewise be responsible for the memory impairment. These additional neural changes could have resulted from direct impact of the hypoxia-ischemia insult and treatments or to plastic changes following early hippocampal atrophy. While this question remains unresolved in the clinical literature, experimental lesion studies in nonhuman primates could provide important clues on the source of the widespread cognitive and neural impacts of neonatal hippocampal damage.

Like the memory impairment reported in children with perinatal hippocampal atrophy, recent reports on the effects of neonatal hippocampal lesions in nonhuman primates (NHPs) have indicated severe and long-lasting deficits in relational memory processes known to be mediated by the hippocampus (Eichenbaum, 2003; O'Keefe and Nadel, 1978; Squire et al., 2007). These deficits include impairment in object recognition memory (Zeamer and Bachevalier, 2013; Zeamer et al., 2010), memory for food/place associations (Glavis-Bloom et al., 2013), and memory for spatial locations and object/place associations (Blue et al., 2013). Interestingly, the neonatal hippocampal lesions appeared to have altered widespread neural systems given that the same animals also presented with loss of working memory processes (Heuer and Bachevalier, 2011a, 2013) thought to be mediated by the lateral prefrontal cortex (Curtis and D'Esposito, 2004; Owen, 2000; Petrides, 2005). Direct evidence of such large scale neural reorganization after early hippocampal lesions in the monkeys has not been fully explored. Earlier studies demonstrated significant changes in the maturation of prefrontal neurons after neonatal medial temporal lobe lesions (Bertolino et al., 1997; Chlan-Fourney et al., 2000; Chlan-Fourney et al., 2003). However, these neural alterations could not be entirely associated with damage to the hippocampus since the neonatal lesions were large, including not only the hippocampus but also the amygdala and adjacent cortical areas. Therefore, the impact of selective neonatal hippocampal lesions on brain functions and microstructure in monkeys remains to be fully investigated. As a first step towards investigating the long range neural changes that may have resulted from early damage to the hippocampus, the present study assessed the integrity of the hippocampal

projections in monkeys that had received bilateral damage to the hippocampus in the first week of life using Diffusion Tensor Imaging (DTI).

DTI is a valuable tool for investigating microstructural integrity and connectivity of neuronal fibers non-invasively, providing a possible biomarker of disease progression and a robust approach to investigate the neuronal substrates for abnormal behaviors of animals and humans. Several useful measures based on DTI have found to be sensitive to a series of white matter-related disruptions in the brain (Le Bihan et al., 2001). For example, fractional anisotropy (FA), a scalar measure of the degree of anisotropic water diffusion of brain tissues, and mean diffusivity (MD) that characterizes the overall displacement of water molecules, are thought to relate to the microstructural features of white-matter organization (Beaulieu, 2002). In addition, recent studies have shown that the three eigenvalues of the diffusion tensor matrix can be further separated into components parallel and perpendicular to local axon tracts, with the former defined as axial diffusivity (D_a) and the average of the latter two defined as radial diffusivity (D_r). D_a and D_r are suggested to indicate different patterns of underlying pathological alterations, such as the disruption and loss of axonal membranes and myelin in the fiber tracts in the brain and also the alterations in the size, density and organization of axons (Le Bihan, 2003; Song et al., 2003; Song et al., 2002). Thus, the patterns of directional diffusivity alteration may be useful in further revealing the nature of white matter disruptions resulting from neonatal hippocampal lesions, and could provide more sensitive measures to explain behavioral and cognitive changes reported after such early lesions.

DTI has been applied to evaluate changes in the white matter microstructure in diseases related to hippocampal damage in human and NHP models (Kubicki et al., 2007; Lee et al., 2012; Shamy et al., 2010). In particular, abnormal FA and diffusivity changes were observed in the fornix and ventromedial prefrontal cortex of macaque monkeys with hippocampal lesions received in adulthood (Shamy et al., 2010). This report suggested that hippocampal damage acquired in adulthood results in altered connections between the hippocampus and cortical regions through the fornix. Given the greater reorganization of brain connectivity usually found after early-onset versus adult-onset brain insults (Kolb et al., 2010; Payne and Cornwell, 1994), it is likely that alterations in the connectional networks of the hippocampus may also be present, or even more pronounced, after early-onset lesions. To test this hypothesis, we performed several processing analyses of DTI data obtained on animals with neonatal hippocampal lesions and their controls, in which detailed behavioral and cognitive characterization was obtained throughout development. Tract-based spatial statistics (TBSS) performs medium-resolution nonlinear registration followed by projection onto an alignment-invariant tract representation, which is a robust and sensitive approach for voxelwise multiple-subject comparisons of DTI data (Smith et al., 2006). This analysis was used to evaluate the integrity of the main hippocampal projection of adult monkeys with neonatal hippocampal lesions and their age-matched controls. To compare and further validate the results, evaluation of white matter changes was performed on the areas of the hippocampal projections by volume of interest analysis, and on the delineated fiber tracts connecting hippocampus and ventromedial prefrontal cortex by probabilistic diffusion tractography performed on the DTI data with high angular resolutions (Behrens et al., 2007; Behrens et al., 2003). Finally, to examine whether the enduring recognition and working

memory deficits after neonatal hippocampal lesions were related to changes in areas onto which the hippocampus projects, correlation analysis was performed between recognition and working memory scores and the DTI-derived measures.

Methods and materials

Animals

Ten adult rhesus macaques (*Macaca mulatta*) of both sexes and aged 8 to 10 years were utilized. Five had received neurotoxic lesions of the hippocampus (Group Neo-Hibo: 3 males, 2 females), induced with bilateral injections of ibotenic acid (5.0 μl) at the age of 10–12 days, and five age-matched controls had received sham lesions (Group Neo-C: 2 males, 3 females). Details of the MRI-guided surgical procedures, lesion evaluation and rearing conditions were reported previously (Goursaud and Bachevalier, 2007; Zeamer et al., 2010). Development of cognitive functions was evaluated in the same cohorts of animals at different time points during development and included measures of object recognition memory (Heuer and Bachevalier, 2011a; Zeamer and Bachevalier, 2013; Zeamer et al., 2010), memory for location and object/place associations (Blue et al., 2013), memory for food/place associations (Glavis-Bloom et al., 2013) and working memory (Heuer and Bachevalier, 2011b, 2013).

Neuroimaging procedures

All procedures were approved and applied in full compliance with the Institutional Animal Care and Use Committees (IACUC) of Emory University, and were in line with the policies outlined in the NRC Guide for the care and use of laboratory animals (2001, 8th ed).

For the scanning procedures, animals were anesthetized with 1–1.5% isoflurane mixed with 100% O_2 and immobilized in a supine position in a custom-made head holder. Et-CO_2, inhaled CO_2, O_2 saturation, blood pressure, heart rate, respiration rate, and body temperature were monitored continuously and body temperature was maintained with a warm blanket surrounding the animal as described previously (Li et al., 2013). An intravenous drip of 0.45% dextrose and sodium chloride was administrated to ensure normal hydration.

All MRI experiments were performed on a Siemens 3T Trio scanner (Siemens Medical Solutions USA, Inc., Malvern, PA). Diffusion images were acquired with a Siemens 8-channel phased-array volume coil and a dual spin-echo, echo planar imaging (EPI) sequence with GRAPPA (R = 3) and the following imaging parameters: TE = 96 ms, TR = 5700 ms, FOV = 96 mm × 96 mm, data matrix = 74 × 74, voxel size = 1.3 mm × 1.3 mm × 1.3 mm. DTI data were collected at a single b-value of 1000 s/mm^2 with 60 diffusion encoding directions chosen to be approximately isotropically distributed on a sphere according to the electrostatic repulsion model (Jones et al., 1999). We acquired 5 repetitions of DTI data sets with the phase-encoding direction in the anterior-posterior (A-P) axis and another 5 repetitions with identical imaging parameters except for reversed phase-encoding direction (P-A) for correcting susceptibility-related distortion with TOPUP function in FSL (Andersson et al., 2003). Each 5 repetitions with the identical phase-encoding direction were co-registered using rigid-body affine transformation and then averaged to improve the signal

to noise ratio (SNR). T_1-weighted images were acquired by using a 3D MPRAGE sequence with GRAPPA (R = 2) with the following parameters: inversion time = 950 ms, TE / TR = 3.5 ms / 3000 ms, FOV = 96 mm × 96 mm, matrix = 192 × 192, 6 averages, and were used for structural identification and to construct an anatomical macaque template for the DTI image registration.

Volumetric measurements of hippocampus

Volumetric measurements of the hippocampus were performed using high-resolution T_1 weighted images and were recorded for the left and right hemispheres separately (Fig. 1). All images containing the hippocampus were identified and selection of the boundaries of the hippocampus were performed with reference to a rhesus macaque brain atlas (Saleem and Logothetis, 2006). The anterior border of the hippocampal formation was the image following that of the most posterior border of the amygdala and was usually the first image posterior to the optic chiasm. This coronal image typically showed the optic tracts splitting away from the optic chiasm and moving to a more lateral position. In this image, the hippocampus is located ventral to the amygdala, and often the tail of the lateral ventricle is visible on the lateral and superior aspects of the hippocampus. The most posterior measurement for the hippocampus was made on the image that clearly showed the crus of the fornix emerging from the hippocampus. On this image, the gyrus fasciolaris and the fornix were excluded from the measurements. On all images between these two extremes, the boundaries of the hippocampus were defined ventrally and medially by the white matter separating the hippocampus from the parahippocampal gyrus. Laterally and dorsally, the borders of the hippocampus followed the temporal horn of the lateral ventricle. Thus, the volume of the hippocampus included the CA fields, dentate gyrus, and subicular complex, but excluded the entorhinal, perirhinal, and parahippocampal cortices. Once all surface area measurements were collected, the volume of the hippocampal formation was calculated for the left and right hemispheres separately (in mm^3) using Cavalieri's principle (Gundersen and Jensen, 1987). Two-way ANOVA with Group (Neo-C and Neo-Hibo) as the between-subject factor and hemisphere (left and right) as the within-subject factor was performed to test differences in hippocampal volumes between hemispheres. P-values less than 0.05 were considered statistically significant.

TBSS analysis

Data were processed with FSL (FMRIB, Oxford) and in-house MATLAB (Mathworks, Natick, MA) scripts. Voxelwise TBSS analysis was derived with FA using the TBSS toolbox in FSL. Specially, FA maps were nonlinearly registered to a population-specific FA template, and then skeletonized (i.e., thining non-maximal FA values perpendicular to the local tract structure) to produce a skeleton mean FA map representing the major white matter tracts with low inter-subject variability. Then, each subject's registered FA image was projected onto the skeleton by filling the skeleton with FA values from the nearest relevant tract center through searching the surface perpendicular to the local skeleton structure (Smith et al., 2006). After confirming normal distribution of the data by a one-sample Kolmogorov-Smirnov test, a two student's sample t-tests was used to *voxelwisely* test the difference within the skeletonized FA maps of the main hippocampal projections, with false discovery rate (FDR) multiple comparisons correction with a q-value of 0.05. The

hippocampal projections include corpus callosum (CC), fornix (FX), temporal stem (TS), optic radiations (OR), cingulum bundle (CB), and ventromedial prefrontal cortex (VM), defined on the basis of atlas of the rhesus monkey brain (Saleem and Logothetis, 2006).

In order to further investigate the underlying mechanisms of the FA changes observed by voxelwise TBSS method, maps of diffusivity indices including mean diffusivity (MD), axial diffusivity (D_a) and radial diffusivity (D_r) were nonlinearly registered to a population-specific template based on the registrations between subjects and the template derived earlier using FA maps, and then skeletonized to produce the skeletons of the corresponding maps. Independent ttests were performed to investigate changes of DTI-derived measures (FA, MD, D_a, D_r) in the areas identified with FA abnormalities using SPSS 17 (SPSS Inc, Chicago, IL, USA). A statistical significance level of $p < 0.05$ was used.

Volume-of-interest analysis

To compare with the TBSS results, DTI-derived measures (i.e., FA, MD, Da, Dr) within the volume of interest of the skeletonised hippocampal projections, including CC, FX, TS, OR, CB and VM, were extracted based on the brain atlas of rhesus monkey (Saleem and Logothetis, 2006). These specific volumes were previously selected to assess the impact of adult-onset hippocampal lesions on white matter in the previous study (Shamy et al., 2010). Independent t-tests were performed on these DTI-derived measures with $p < 0.05$ significance level.

Analysis of fiber tracts connecting hippocampus and VM

To further validate the alterations of the structural connections between hippocampus and ventromedial prefrontal cortex, probabilistic tractography was used to track the fiber tracts connecting the hippocampus and ventromedial prefrontal cortex, implemented with FSL (Behrens et al., 2007; Behrens et al., 2003). These two areas, defined on the basis of the rhesus monkey brain atlas (Saleem and Logothetis, 2006), were exacted from the T_1-weighted brain template. The two areas were then aligned to the native diffusion space to conduct the fiber tracking for each individual. Probabilistic tractography was carried out in two-mask mode (i.e., the two areas of hippocampus and ventromedial prefrontal cortex) with a waypoint mask of fornix or temporal stem. In this way, only the tracts passing through the fornix or temporal stem between two seed regions were kept and delineated. 5000 samples from each voxel in the seed masks were sent to generate a map of streamline hits connecting the two seed masks. The probabilistic map of connectivity in each individual was further normalized by the number of samples that were sent from the seed mask and reached the other seed mask (i.e., waytotal), and then was transformed to the T1-weighted template using nonlinear transformation. The normalized connectivity maps from all animals were subsequently averaged across animals for a probability map in the population. The final population-specific tracts connecting the hippocampus and the ventromedial prefrontal cortex were generated by thresholding the results at 0.1% before the binarization. We then extracted the DTI-derived measures (FA, MD, D_a, D_r) on the skeleton of the tracts of each subject using these tract-defined volume-of-interests specific to the VM-hippocampus pathway. Independent t-tests were performed to test group difference in these measures with $p < 0.05$ significance level.

Correlation analysis with behavioral measures

Pearson's correlation analysis in the Neo-Hibo group was carried out to evaluate the relation between with the memory scores in recognition and working memory tasks (Heuer and Bachevalier, 2013; Zeamer and Bachevalier, 2013) and the DTI-derived measures with significant group difference revealed by TBSS analysis, volume-of-interest analysis, and tracts-defined analysis, as stated above. For the incidental object recognition task (Zeamer and Bachevalier, 2013), memory scores were represented by the percent looking at novel black-white pictures at delays of 120-s collected at 48 months of age (n = 4). In the 4-objects serial order working memory task (SMOT) (Heuer and Bachevalier, 2013), memory scores were ratio scores measuring cumulative correct responses on the inner object discrimination (2 vs 3) divided by the number of correct responses on the outer discrimination (1 vs 4) across the three-day probe sessions collected at 6 and 8 years of age (n = 5). Higher scores indicated better performance. P-values less than 0.05 were considered statistically significant.

Results

Volumetric measurements results for hippocampus

As expected, there was a significant difference between groups in hippocampal volume ($F(1, 16) = 21.15$, $p < 0.0001$), confirming that the volume of the hippocampus was significantly smaller in monkeys that had received neonatal neurotoxic injections than in controls. However, differences between hemispheres were not significant ($F(1, 16) = 0.32$, $p = 0.58$) nor was the interaction between group and hemisphere ($F(1, 16) = 0.061$, $p = 0.81$).

TBSS analysis results

The voxelwise TBSS analysis revealed several brain areas with significant FA difference of the hippocampal projections in Neo-Hibo animals relative to Neo-C animals (Fig. 2). These areas included the fornix, ventromedial prefrontal cortex (see z = 0.0 mm, 2.5 mm in Fig. 2), optic radiations, and the left temporal stem. In addition to changes in FA values, the diffusivity indices also showed alterations in these same regions. As shown in Table 1, significant increases in MD and D_r were found in the left TS and in both hemispheres for FX; significant increase in D_r was found in the left VM, and in both hemispheres for OR.

Volume-of-interest analysis results

The volume-of-interest analysis (Table 1) showed several changes in FA values and diffusivity indices. These changes included: a) significant decrease in FA and increase in MD and D_r in FX of both hemispheres (all p values < 0.05); b) a trend in increased MD ($p = 0.06$) and a significant increase in D_r ($p = 0.048$) in the left VM; and c) a significant increase in MD ($p = 0.037$) and D_r ($p = 0.048$) in the left TS. No change of FA or diffusivity indices was found in other areas ($p > 0.1$).

Results of analysis of fiber tracts connecting hippocampus and VM

As expected (see Table 1), significant changes in DTI-derived measures were also found in tracts connecting hippocampus and VM (Fig. 3 and Fig. 4). Animals with neonatal hippocampal lesions showed decreased FA ($p < 0.05$), increased MD ($p < 0.05$) and D_r ($p < 0.05$) in the fibers passing through FX and reaching the VM in both hemispheres. In addition, significant increase in D_r ($p = 0.035$) was found in the fiber tract passing through TS in the left hemisphere and reaching the left VM.

Correlation analysis results

As shown in Table 2 and Fig. 5, D_r values in the FA-identified regions in the left VM were negatively correlated with the working memory scores ($p < 0.03$), though such significant correlation would not hold up to FDR correction with q-value = 0.05. No significant correlations between the working memory scores and the DTI-derived measures were observed in all other areas identified by either TBSS analysis, volume-of-interest analysis or analysis based on the fiber tracts connecting hippocampus and VM. There were no any significant correlations between the incidental recognition memory scores and any DTI-derived measures (see Table 2, $p \geq 0.08$).

Discussion

The present study demonstrates significant and enduring alterations of white matter integrity in the hippocampal projections of adult monkeys with neonatal hippocampal lesions. These white matter changes were observed not only in the fornix and ventromedial prefrontal cortex, as for the adult-onset lesions (Shamy et al., 2010), but also in the temporal stem and optic radiations. Although the white matter changes in the hippocampal projections did not correlated with recognition memory performance, white matter microstructural alterations in the left ventromedial prefrontal cortex significantly correlated with the working memory deficits reported in the same animals.

Analysis of results and possible mechanism for the change of DTI-derived measures

DTI-derived measures were compared and validated by using TBSS analysis, volume-ofinterest analysis, and tracts-defined analysis. TBSS analysis on DTI-derived metrics is more sensitive than volume-of-interest analysis as TBSS allows voxelwise comparisons of maximal DTI-derived measures on the skeleton maps, avoiding inter-rater variability and averaging FA values over a large region of interests (Smith et al., 2006). In the present study, TBSS analysis revealed significant differences of more DTI-derived measures and in more areas of the hippocampal projections measured. For example, both decreased FA and increased D_r were found in the left VM by TBSS analysis, whereas only increased D_r was found in the left VM when using volume-of-interest analysis. Similar differences between the two analyses were found in the left TS and the left and right OR, where fewer or no changes in the DTI-derived measures were detected with volume-of-interest analysis, as compared to TBSS analysis. The undetectable DTI-derived measures in OR by volume-of-interest analysis suggest that changes in OR may be restricted to only a portion, but not the entire, part of this fiber tract.

FA, MD, Da and Dr are scalar measures based on simplistic diffusion tensor model where only one dominant diffusion direction is assumed in each voxel. A recent study indicates that 63~90% of brain white matter contains more than one fiber bundle with different orientations (Jeurissen et al., 2013). To further examine if the fiber-crossing effects hinder the detectability of white matter microstructure changes between Neo-C and Neo-Hibo animals, we further performed TBSS analyses based on a multi-fiber model (Behrens et al., 2007), in which the diffusion signal is decomposed into multiple fiber orientations in a single voxel(see Supplemental Materials). Therefore, measuring contribution of each fiber orientation to the diffusion MR signal is more interpretable than using the conventional DTI-derived measures in the regions with crossing fibers (Jbabdi et al., 2010). As shown in Table A.1 (Supplemental Materials), decreased compartmental fraction (either f1 or f2) was observed in left TS, and also VM, FX and OR in both hemispheres, whereas no changes of f1 or f2 were seen in other hippocampal projectional areas. These results are in good agreement with those in Table 1, indicating the findings of general TBSS analysis may not be affected significantly with the crossing fibers.

Nevertheless, FX and the left VM showed significant decreased FA, and/or increased MD and D_r detectable with both TBSS and volume-of-interest analysis, suggesting extensive changes in these two areas. We further performed tract-defined analyses, which confirmed the findings detected with the TBSS and volume-of-interest methods. As expected, the tracts connecting hippocampus and VM passing through fornix showed significant decrease in FA and increase in MD and D_r in both hemispheres, and the tracts connecting hippocampus and VM via TS showed significant increases in D_r in the left hemisphere. TS includes fibers from the uncinate fasciculus connecting the anterior temporal cortical regions to the gyrus rectus (VM) as well as medial and lateral orbital gyri (Thiebaut de Schotten et al., 2012).

FA changes in white matter could be attributed to alterations of myelination, axon size, fiber geometry and extracellular water space (Le Bihan, 2003). The finding of significant increase in D_r is consistent with the axonal injury and also in adult-onset hippocampal lesion model reported previously, which is probably due to disruption of the integrity of myelin sheaths in these affected areas and fiber tracts (Concha et al., 2006; Shamy et al., 2010; Song et al., 2002).

Widespread white matter microstructural changes

The fornix represents one of the main outputs originating from the hippocampus (Rosene and Van Hoesen, 1977) and, as expected, most DTI parameters (i.e., FA, MD, D_r) in this fiber tract were significantly altered in Neo-Hibo animals as compared to controls. These alterations are indicative of changes in the integrity of the axonal projections and/or myelin sheaths (Concha et al., 2006; Song et al., 2002), and are consistent with similar changes previously reported in macaques that had received neurotoxic hippocampal lesions in adulthood (Shamy et al., 2010). The present study extends these earlier data by demonstrating that the white matter microstructural changes in the fornix are present even when damage to the hippocampus occurs early in infancy and are consistent with recent findings in infant monkeys demonstrating the presence of ammonic and subicular neurons at birth (Jabès et al., 2010, 2011; Lavenex and Banta Lavenex, 2013) constituting the origins of

hippocampal efferent fibers coursing through the fornix. In addition, similar to adult-onset hippocampal lesions (Shamy et al., 2010), white matter abnormalities in the fornix following neonatal hippocampal lesions were associated with white matter changes in ventromedial prefrontal cortex onto which the hippocampal-fornix efferent fibers terminate (Cavada et al., 2000; Croxson et al., 2005). Thus, FA reduction in VM was consistent with the D_r increase.

There were two additional white matter changes in the optic radiations and the temporal stem after the neonatal hippocampal lesions that were not reported previously in animals with adult-onset hippocampal lesions (Shamy et al., 2010). These white matter changes were present in the optic radiations and the temporal stem as indicated by decreased FA and increased D_r in each fiber tract. These different outcomes may relate to the type of DTI analyses performed, given that, as the earlier report, we found fewer changes in DTI indices in these two tracts when using volume-of-interest than when using the more sensitive TBSS analysis. Both OR and TS are not directly connected with the hippocampus but contain fibers from temporal cortical areas with which the hippocampus has strong anatomical projections. For example, OR contains fibers connecting the occipital cortical areas to the parahippocampal gyrus via the inferotemporal segment of inferior longitudinal fasciculus (Schmahmann and Pandya, 2006) and TS contains fibers from the medial temporal cortical areas to the ventral prefrontal cortex via the uncinate fasciculus (Choi et al., 2010; Croxson et al., 2005; Ebeling and von Cramon, 1992; Kier et al., 2004; Schmahmann and Pandya, 2006; Ungerleider et al., 1989). Thus, the impact of early insult to the hippocampus on OR and TS white matter may have resulted from unintended damage to these medial temporal cortical areas, i.e. parahippocampal areas TH/TF for OR changes and entorhinal and perirhinal cortex for TS changes. This possibility seems unlikely, however, given that careful inspection of the extent of hypersignals seen on the anatomical MR FLAIR images taken 1 week after the neurotoxic injections (see Table 2 and Fig. 2 in (Goursaud and Bachevalier, 2007)) indicated negligible damage to these cortical areas (average: 5.4 % for area TH/TF, 0.3% and 0.5% for the entorhinal and perirhinal cortex). Furthermore, sparing of these temporal cortical areas after neonatal hippocampal lesions was also seen on the high-resolution structural T_1 images acquired at the same time of the DTI scans (see illustration on Fig. 1 for 2 cases).

The sensitivity of TBSS analysis to detect white matter changes was also demonstrated by the correlation analysis. As shown in Table 2, the radial diffusivity (D_r) in VM identified only with TBSS analyses significantly correlated with the memory scores. This correlation is in accordance with the known projections from the hippocampus to VM via the fornix (Cavada et al., 2000; Croxson et al., 2005). It was found that memory performance correlated with DTI indices in VM but not in DTI indices in the fiber tracts connecting the hippocampus to VM. Although the impaired hippocampus altered both the hippocampal projectional pathway and the projected destination, the correlation results emphasis the importance of prefrontal cortex in memory performance, as compared to the pathways connecting hippocampus and the prefrontal cortex.

The most interesting, and perhaps unexpected, finding of the present study was the significant alterations of the white matter within the temporal stem. Changes of DTI-derived measures were found in animals with neonatal hippocampal lesions as compared to controls.

No such changes were previously reported when the hippocampal lesions were acquired in adulthood (Shamy et al., 2010). The temporal stem consists of fibers linking the temporal and frontal lobes via the uncinate fasciculus (Choi et al., 2010; Ebeling and von Cramon, 1992; Kier et al., 2004; Schmahmann and Pandya, 2006; Thiebaut de Schotten et al., 2012; Ungerleider et al., 1989). Fibers coursing through the uncinate fasciculus do not originate directly from hippocampal neurons but rather from temporal cortical areas such as the entorhinal (BA area 28) and perirhinal (BA 35) cortex; two medial temporal cortical areas heavily interconnected with the hippocampus. Thus, the impact of early insult to the hippocampus on temporal stem white matter may also have resulted from unintended damage to these medial temporal cortical areas. This possibility also seems unlikely, however, given that as mentioned above, careful inspection of the extent of hypersignals seen on the anatomical MR FLAIR images taken 1 week after the neurotoxic injections (see Table 2 and Fig. 2 in the previous report (Goursaud and Bachevalier, 2007)) indicated negligible damage to these two cortical areas (average: 0.4% and 0.2% for the left and right entorhinal cortex and 0.9% and 0.2% for the left and right perirhinal cortex).

Another interpretation for the impact of the neonatal lesions on white matter connecting the temporal and frontal lobes may relate to the time course of maturation of white matter fasciculi. Although there exists no such information in monkeys, data in humans suggest that the temporal-prefrontal fiber tracts develop postnatally with the uncinate fasciculus showing the most prolonged maturation (Lebel et al., 2008). Thus, the microstructural changes in the temporal stem may relate to a lack of functional inputs from the hippocampus to the entorhinal and perirhinal cortex at a time in development when axons from these cortical areas are not fully matured. The laterality effect observed in the correlation between DTI changes in VM and working memory scores is intriguing and has also been reported in humans for working memory processes and decision-making, using functional imaging (Gallagher et al., 2000; Goel et al., 1995; Leopold et al., 2012; Oztekin et al., 2009; Tranel et al., 2002). However, a more definite explanation for the asymmetric DTI changes found in the temporal stem will likely be reached upon post-mortem histological analyses of the brain of the animals with neonatal hippocampal lesions.

Relationships to cognitive deficits

The behavioral and cognitive development of the animals participating in this study have been fully characterized using multiple paradigms at different time points and allowed us to consider whether the microstructural changes in hippocampal connections described above may be associated with some of the deficits observed in the same animals. Despite the small sample size, we found that white matter radial diffusivity (D_r) alterations in left ventromedial prefrontal cortex were closely related to the deficits in working memory (Heuer and Bachevalier, 2013). Although no correlations were found between working memory scores and the DTI-derived measures in the temporal stem, the working memory deficits may be associated with microstructural changes in the uncinate fasciculus connecting the anterior temporal cortex to the ventromedial prefrontal cortex as revealed by the increased D_r in TS. This is supported by recent findings in humans demonstrating correlation between DTI indices in the uncinate fasciculus with memory scores (Sato et al., 2012). In the current study, the correlation between microstructural alterations in the left

ventromedial prefrontal cortex and working memory deficits validates the enduring morphological and functional impairments in development of hippocampal-prefrontal connections.

Limitations in the present study

One limitation in this study is the small number of animals available in the lesion model, although such unique model could provide essential information for evaluating the widespread impact of the neonatal hippocampal lesion in adulthood. With the limited sample size, individual variations in DTI-measures resulted in significant group comparisons that could not hold up to FDR correction and more animals would be required to obtain significant p values when comparing multiple regions. Likewise, in the correlation analysis, the significant correlation between Dr of left VM and the serial order working memory scores would not hold up to FDR correction (Table 2). Thus, the alterations in DTI-measures, which were perhaps due to the demyelization of the white matter, could be more convincing after post-mortem brain histological analyses that will be performed after all in vivo examinations are complete.

Conclusion

The study demonstrates widespread disruption of white matter following selective neonatal lesions of the hippocampus. The data provide relevant information for the source of the cognitive and memory deficits reported in developmental cases of ischemic-hypoxic hippocampal damage in humans. Although volumetric gray matter alterations of other brain structures, such as posterior thalamus, putamen and retrosplenial cortex, are also present in these children (Vargha-Khadem et al., 2003), no studies to date have examined white matter integrity of the hippocampal connectional system in these cases. Thus, the present data indicate for the first time that, as for the monkeys, early selective insult to the hippocampus in humans is likely to result in significant white matter alterations in fiber tracts associated with the hippocampus as well as in white matter of the ventromedial prefrontal cortex. These white matter changes may also provide, at least in part, an account for the memory loss reported in the human cases.

Supplementary Material

Refer to Web version on PubMed Central for supplementary material.

Acknowledgments

This project was funded or supported by NIH/NIMH grant MH0588446 (JB), the National Center for Research Resources P51RR000165 and the Office of Research Infrastructure Programs / OD P51OD011132. We would like to thank Sudeep Patel for MRI data acquisition, Ruth Connelly and Doty Kempf (DVM) for their expert assistance with the care of the animals during the neuroimaging procedures.

References

Adlam AL, Malloy M, Mishkin M, Vargha-Khadem F. Dissociation between recognition and recall in developmental amnesia. Neuropsychologia. 2009; 47:2207–2210. [PubMed: 19524088]

Andersson JLR, Skare S, Ashburner J. How to correct susceptibility distortions in spin-echo echo-planar images: application to diffusion tensor imaging. Neuroimage. 2003; 20:870–888. [PubMed: 14568458]

Bachevalier J, Vargha-Khadem F. The primate hippocampus: ontogeny, early insult and memory. Curr. Opin. Neurobiol. 2005; 15:168–174. [PubMed: 15831398]

Bartsch, T. The clinical neurobiology of the hippocampus: An integrative view. Oxford, UK: Oxford University Press; 2012.

Beaulieu C. The basis of anisotropic water diffusion in the nervous system - a technical review. NMR Biomed. 2002; 15:435–455. [PubMed: 12489094]

Behrens TE, Berg HJ, Jbabdi S, Rushworth MF, Woolrich MW. Probabilistic diffusion tractography with multiple fibre orientations: What can we gain? Neuroimage. 2007; 34:144–155. [PubMed: 17070705]

Behrens TE, Woolrich MW, Jenkinson M, Johansen-Berg H, Nunes RG, Clare S, Matthews PM, Brady JM, Smith SM. Characterization and propagation of uncertainty in diffusion-weighted MR imaging. Magn. Reson. Med. 2003; 50:1077–1088. [PubMed: 14587019]

Bertolino A, Saunders RC, Mattay VS, Bachevalier J, Frank JA, Weinberger DR. Altered development of prefrontal neurons in rhesus monkeys with neonatal mesial temporo-limbic lesions: a proton magnetic resonance spectroscopic imaging study. Cereb. Cortex. 1997; 7:740–748. [PubMed: 9408038]

Blue SN, Kazama AM, Bachevalier J. Development of memory for spatial locations and object/place associations in infant rhesus macaques with and without neonatal hippocampal lesions. J. Int. Neuropsychol. Soc. 2013; 19:1053–1064. [PubMed: 23880255]

Cavada C, Company T, Tejedor J, Cruz-Rizzolo RJ, Reinoso-Suarez F. The anatomical connections of the macaque monkey orbitofrontal cortex. A review. Cereb. Cortex. 2000; 10:220–242.

Chlan-Fourney J, Webster MJ, Felleman DJ, Bachevalier J. Neonatal medial temporal lobe lesions alter the distribution of tyrosine hydroxylase immunoreactive varicosities in the macaque prefrontal cortex. Soc. Neurosci. Abstr. 2000; 26:609.

Chlan-Fourney J, Webster MJ, Jung J, Bachevalier J. Neonatal medial temporal lobe lesions decrease GABAergic interneuron densities in macaque prefrontal cortex: Implications for schizophrenia and Autism. Soc. Neurosci. Abstr. 2003; 29

Choi CY, Han SR, Yee GT, Lee CH. A understanding of the temporal stem. J. Korean Neurosurg. Soc. 2010; 47:365–369. [PubMed: 20539796]

Concha L, Gross DW, Wheatley BM, Beaulieu C. Diffusion tensor imaging of time-dependent axonal and myelin degradation after corpus callosotomy in epilepsy patients. Neuroimage. 2006; 32:1090–1099. [PubMed: 16765064]

Croxson PL, Johansen-Berg H, Behrens TE, Robson MD, Pinsk MA, Gross CG, Richter W, Richter MC, Kastner S, Rushworth MF. Quantitative investigation of connections of the prefrontal cortex in the human and macaque using probabilistic diffusion tractography. J. Neurosci. 2005; 25:8854–8866. [PubMed: 16192375]

Curtis CE, D'Esposito M. The effects of prefrontal lesions on working memory performance and theory. Cogn. Affect. Behav. Neurosci. 2004; 4:528–539. [PubMed: 15849895]

de Haan M, Mishkin M, Baldeweg T, Vargha-Khadem F. Human memory development and its dysfunction after early hippocampal injury. Trends Neurosci. 2006; 29:374–381. [PubMed: 16750273]

Ebeling U, von Cramon D. Topography of the uncinate fascicle and adjacent temporal fiber tracts. Acta Neurochir. 1992; 115:143–148. [PubMed: 1605083]

Eichenbaum H. How does the hippocampus contribute to memory? Trends Cogn. Sci. 2003; 7:427–429. [PubMed: 14550483]

Gadian DG, Aicardi J, Watkins KE, Porter DA, Mishkin M, Vargha-Khadem F. Developmental amnesia associated with early hypoxic-ischaemic injury. Brain. 2000; 123(Pt 3):499–507. [PubMed: 10686173]

Gallagher HL, Happe F, Brunswick N, Fletcher PC, Frith U, Frith CD. Reading the mind in cartoons and stories: an fMRI study of 'theory of mind' in verbal and nonverbal tasks. Neuropsychologia. 2000; 38:11–21. [PubMed: 10617288]

Glavis-Bloom C, Alvarado MC, Bachevalier J. Neonatal hippocampal damage impairs specific food/place associations in adult macaques. Behav. Neurosci. 2013; 127:9–22. [PubMed: 23398438]

Goel V, Grafman J, Sadato N, Hallett M. Modeling other minds. Neuroreport. 1995; 6:1741–1746. [PubMed: 8541472]

Goursaud AP, Bachevalier J. Social attachment in juvenile monkeys with neonatal lesion of the hippocampus, amygdala and orbital frontal cortex. Behav. Brain Res. 2007; 176:75–93. [PubMed: 17084912]

Gundersen HJ, Jensen EB. The efficiency of systematic sampling in stereology and its prediction. J. Microsc. 1987; 147:229–263. [PubMed: 3430576]

Heuer E, Bachevalier J. Effects of selective neonatal hippocampal lesions on tests of object and spatial recognition memory in monkeys. Behav. Neurosci. 2011a; 125:137–149. [PubMed: 21341885]

Heuer E, Bachevalier J. Neonatal hippocampal lesions in rhesus macaques alter the monitoring, but not maintenance, of information in working memory. Behav. Neurosci. 2011b; 125:859–870. [PubMed: 21928873]

Heuer E, Bachevalier J. Working memory for temporal order is impaired after selective neonatal hippocampal lesions in adult rhesus macaques. Behav. Brain Res. 2013; 239:55–62. [PubMed: 23137699]

Jabès A, Lavenex PB, Amaral DG, Lavenex P. Quantitative analysis of postnatal neurogenesis and neuron number in the macaque monkey dentate gyrus. Eur. J. Neurosci. 2010; 31:273–285. [PubMed: 20074220]

Jabès A, Lavenex PB, Amaral DG, Lavenex P. Postnatal development of the hippocampal formation: a stereological study in macaque monkeys. J. Comp. Neurol. 2011; 519:1051–1070. [PubMed: 21344402]

Jbabdi S, Behrens TE, Smith SM. Crossing fibres in tract-based spatial statistics. Neuroimage. 2010; 49:249–256. [PubMed: 19712743]

Jeurissen B, Leemans A, Tournier JD, Jones DK, Sijbers J. Investigating the prevalence of complex fiber configurations in white matter tissue with diffusion magnetic resonance imaging. Hum. Brain Mapp. 2013; 34:2747–2766. [PubMed: 22611035]

Jones DK, Horsfield MA, Simmons A. Optimal strategies for measuring diffusion in anisotropic systems by magnetic resonance imaging. Magn. Reson. Med. 1999; 42:515–525. [PubMed: 10467296]

Kier EL, Staib LH, Davis LM, Bronen RA. MR imaging of the temporal stem: anatomic dissection tractography of the uncinate fasciculus, inferior occipitofrontal fasciculus, and Meyer's loop of the optic radiation. AJNR Am. J. Neuroradiol. 2004; 25:677–691. [PubMed: 15140705]

Kolb, B.; Halliwell, C.; Gibb, R. Factors influencing neocortical development in the normal and injured brain. In: Blumberg, MS.; Freeman, JH.; Robinson, SR., editors. Oxford Handbook of Developmental Behavioral Neuroscience. New York: Oxford University Press; 2010.

Kubicki M, McCarley R, Westin CF, Park HJ, Maier S, Kikinis R, Jolesz FA, Shenton ME. A review of diffusion tensor imaging studies in schizophrenia. J. Psychiat. Res. 2007; 41:15–30. [PubMed: 16023676]

Lavenex P, Banta Lavenex P. Building hippocampal circuits to learn and remember: insights into the development of human memory. Behav. Brain Res. 2013; 254:8–21. [PubMed: 23428745]

Le Bihan D. Looking into the functional architecture of the brain with diffusion MRI. Nat. Rev. Neurosci. 2003; 4:469–480. [PubMed: 12778119]

Le Bihan D, Mangin JF, Poupon C, Clark CA, Pappata S, Molko N, Chabriat H. Diffusion tensor imaging: Concepts and applications. J. Magn. Reson. Imaging. 2001; 13:534–546. [PubMed: 11276097]

Lebel C, Walker L, Leemans A, Phillips L, Beaulieu C. Microstructural maturation of the human brain from childhood to adulthood. Neuroimage. 2008; 40:1044–1055. [PubMed: 18295509]

Lee DY, Fletcher E, Carmichael OT, Singh B, Mungas D, Reed B, Martinez O, Buonocore MH, Persianinova M, DeCarli C. Sub-regional hippocampal injury is associated with fornix degeneration in Alzheimer's disease. Front. Aging Neurosci. 2012; 4

Leopold A, Krueger F, dal Monte O, Pardini M, Pulaski SJ, Solomon J, Grafman J. Damage to the left ventromedial prefrontal cortex impacts affective theory of mind. Soc. Cogn. Affect. Neurosci. 2012; 7:871–880. [PubMed: 22021651]

Li CX, Patel S, Auerbach EJ, Zhang X. Dose-dependent effect of isoflurane on regional cerebral blood flow in anesthetized macaque monkeys. Neurosci. Lett. 2013; 541:58–62. [PubMed: 23428509]

O'Keefe, J.; Nadel, L. The hippocampus as a cognitive map. Oxford University Press; 1978.

Owen AM. The role of the lateral frontal cortex in mnemonic processing: the contribution of functional neuroimaging. Exp. Brain Res. 2000; 133:33–43. [PubMed: 10933208]

Oztekin I, McElree B, Staresina BP, Davachi L. Working memory retrieval: contributions of the left prefrontal cortex, the left posterior parietal cortex, and the hippocampus. J. Cogn. Neurosci. 2009; 21:581–593. [PubMed: 18471055]

Payne BR, Cornwell P. System-wide repercussions of damage to the immature visual cortex. Trends Neurosci. 1994; 17:126–130. [PubMed: 7515529]

Petrides M. Lateral prefrontal cortex: architectonic and functional organization. Philos. Trans. R. Soc. Lond. B Biol. Sci. 2005; 360:781–795. [PubMed: 15937012]

Rosene DL, Van Hoesen GW. Hippocampal efferents reach widespread areas of cerebral cortex and amygdala in the rhesus monkey. Science. 1977; 198:315–317. [PubMed: 410102]

Saleem, KS.; Logothetis, NK. A combined MRI and histology atlas of the rhesus monkey brain in stereotaxic coordinates. Academic Press; 2006.

Sato T, Maruyama N, Hoshida T, Minato K. Correlation between uncinate fasciculus and memory tasks in healthy individual using diffusion tensor tractography. Conf. Proc. IEEE Eng. Med. Biol. Soc. 2012; 2012:424–427. [PubMed: 23365919]

Schmahmann, JD.; Pandya, DN. Fiber pathways of the brain. New York: Oxford University Press; 2006.

Shamy JL, Carpenter DM, Fong SG, Murray EA, Tang CY, Hof PR, Rapp PR. Alterations of white matter tracts following neurotoxic hippocampal lesions in macaque monkeys: a diffusion tensor imaging study. Hippocampus. 2010; 20:906–910. [PubMed: 20095006]

Smith SM, Jenkinson M, Johansen-Berg H, Rueckert D, Nichols TE, Mackay CE, Watkins KE, Ciccarelli O, Cader MZ, Matthews PM, Behrens TE. Tract-based spatial statistics: voxelwise analysis of multi-subject diffusion data. Neuroimage. 2006; 31:1487–1505. [PubMed: 16624579]

Song SK, Sun SW, Ju WK, Lin SJ, Cross AH, Neufeld AH. Diffusion tensor imaging detects and differentiates axon and myelin degeneration in mouse optic nerve after retinal ischemia. Neuroimage. 2003; 20:1714–1722. [PubMed: 14642481]

Song SK, Sun SW, Ramsbottom MJ, Chang C, Russell J, Cross AH. Dysmyelination revealed through MRI as increased radial (but unchanged axial) diffusion of water. Neuroimage. 2002; 17:1429–1436. [PubMed: 12414282]

Squire LR, Wixted JT, Clark RE. Recognition memory and the medial temporal lobe: a new perspective. Nat. Rev. Neurosci. 2007; 8:872–883. [PubMed: 17948032]

Thiebaut de Schotten M, Dell'Acqua F, Valabregue R, Catani M. Monkey to human comparative anatomy of the frontal lobe association tracts. Cortex. 2012; 48:82–96. [PubMed: 22088488]

Tranel D, Bechara A, Denburg NL. Asymmetric functional roles of right and left ventromedial prefrontal cortices in social conduct, decision-making, and emotional processing. Cortex. 2002; 38:589–612. [PubMed: 12465670]

Ungerleider LG, Gaffan D, Pelak VS. Projections from inferior temporal cortex to prefrontal cortex via the uncinate fascicle in rhesus monkeys. Exp. Brain Res. 1989; 76:473–484. [PubMed: 2792241]

Vargha-Khadem F, Gadian DG, Watkins KE, Connelly A, Van Paesschen W, Mishkin M. Differential effects of early hippocampal pathology on episodic and semantic memory. Science. 1997; 277:376–380. [PubMed: 9219696]

Vargha-Khadem F, Salmond CH, Watkins KE, Friston KJ, Gadian DG, Mishkin M. Developmental amnesia: effect of age at injury. P. Natl. Acad. Sci. U.S.A. 2003; 100:10055–10060.

Zeamer A, Bachevalier J. Long-term effects of neonatal hippocampal lesions on novelty preference in monkeys. Hippocampus. 2013; 23:745–750. [PubMed: 23640834]

Zeamer A, Heuer E, Bachevalier J. Developmental trajectory of object recognition memory in infant rhesus macaques with and without neonatal hippocampal lesions. J. Neurosci. 2010; 30:9157–9165. [PubMed: 20610749]

Highlights

1. Adult macaques with neonatal hippocampal lesion are investigated with DTI.
2. FA and MD are altered in fornix, temporal stem, prefrontal cortex and optical radiations.
3. Abnormal connections between hippocampus and ventromedial prefrontal cortex are observed.
4. The DTI findings are associated with the cognitive deficits of adult macaques with neonatal hippocampal lesion.

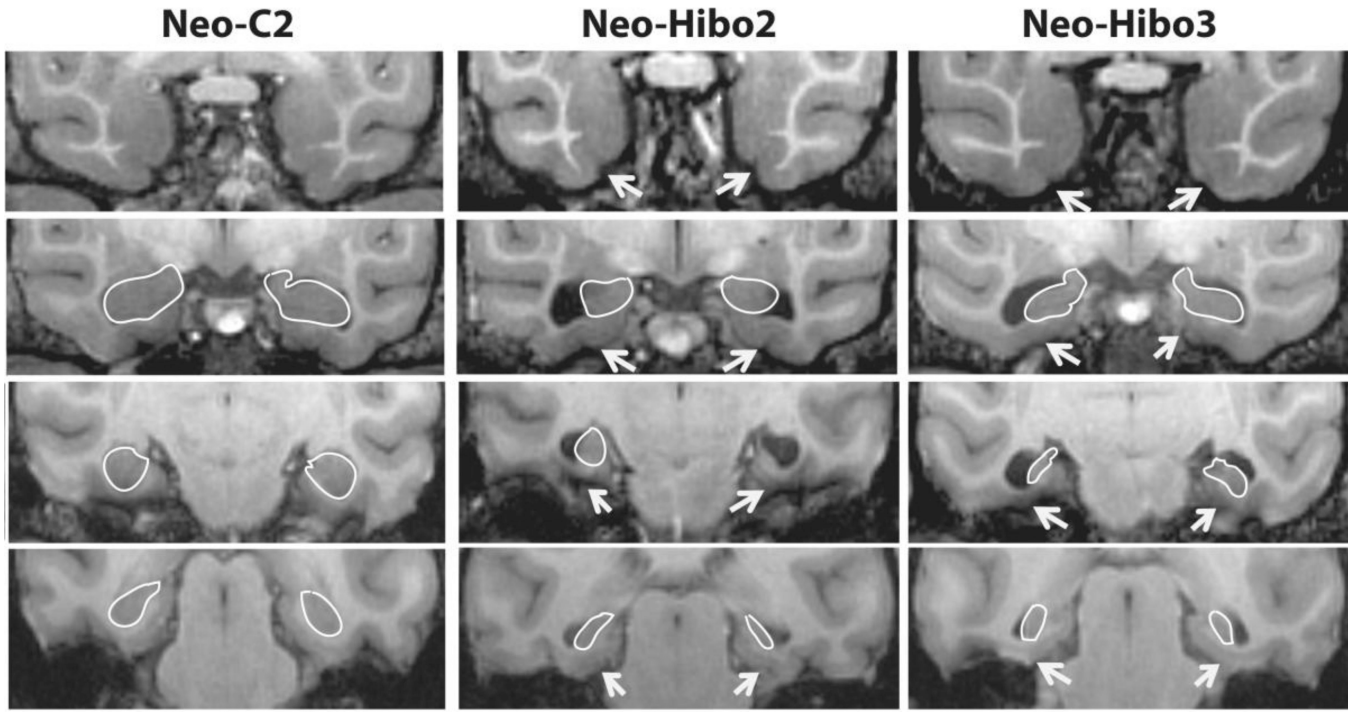

Figure 1.

Coronal T1-weighted images through the rostro-caudal extent of the medial temporal lobe illustrating the loss of hippocampal tissue in cases Neo-Hibo2 and Neo-Hibo3 as compared to a sham-operated control (Neo-C2). The white outlines illustrate the borders of the hippocampal formation in all three cases (see text for a more complete description). White arrows point to sparing of entorhinal (Brodmann area 28), perirhinal (Brodmann areas 35/36), and parahippocampal areas TH/TF cortices in the two representative cases with neurotoxic hippocampal lesions.

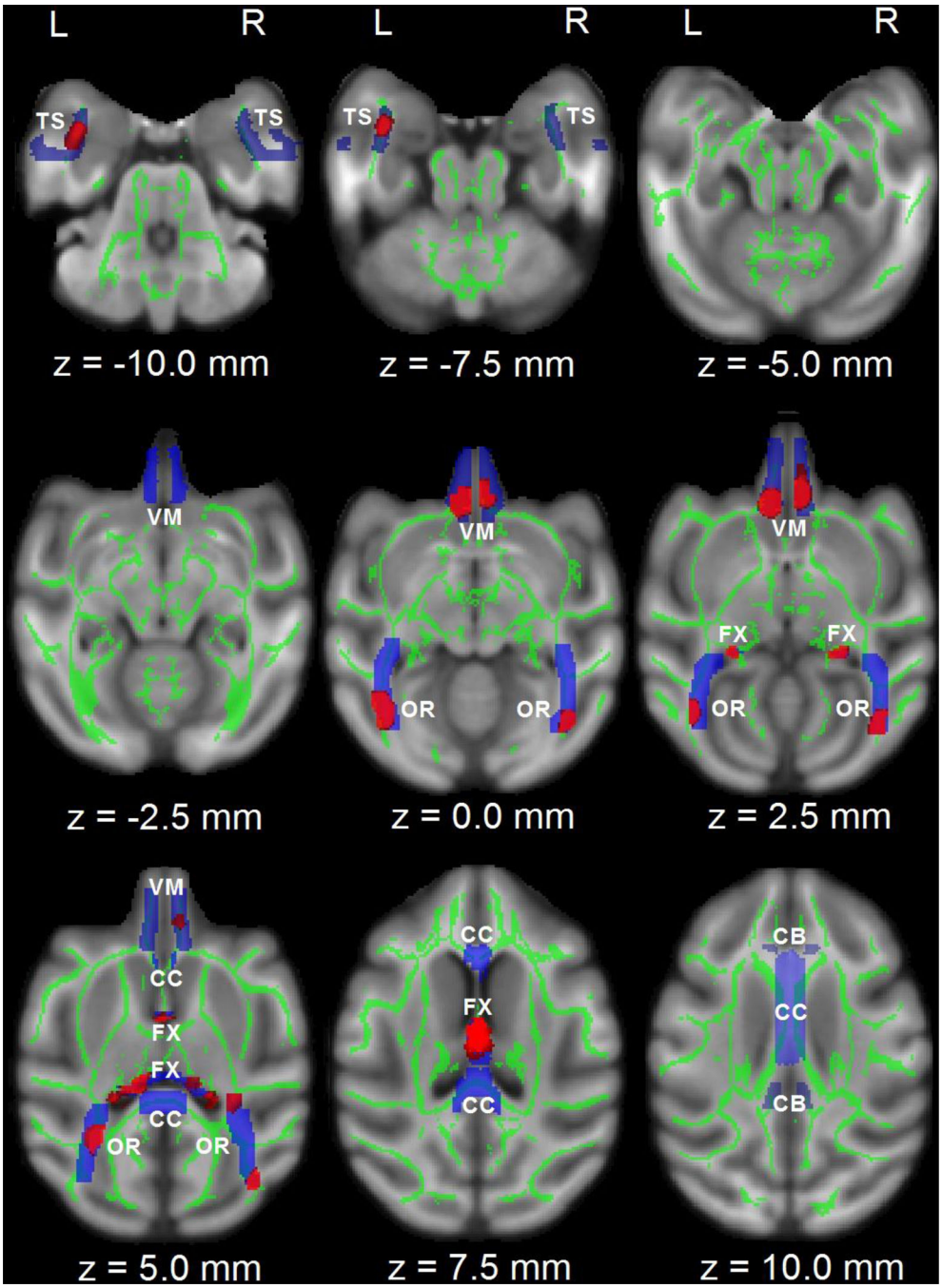

Figure 2.

TBSS and volume-of interest analysis in the hippocampal projections in the horizontal direction (z). Areas with red color indicate significant FA group difference ($p < 0.05$, corrected with FDR). To aid visualization, voxels showing significant difference are thickened using the “tbss_fill” script implemented in FSL. Areas in blue color indicate the hippocampal projectional ROIs. DTI-derived measures within areas were averaged from the correspondent skeletonized map (e.g., FA) in green color. Abbreviation: CC, corpus

callosum; FX, fornix; TS, temporal stem; OR, optic radiations; CB, cingulum bundle; VM, ventromedial prefrontal cortex. L, R: left or right hemisphere.

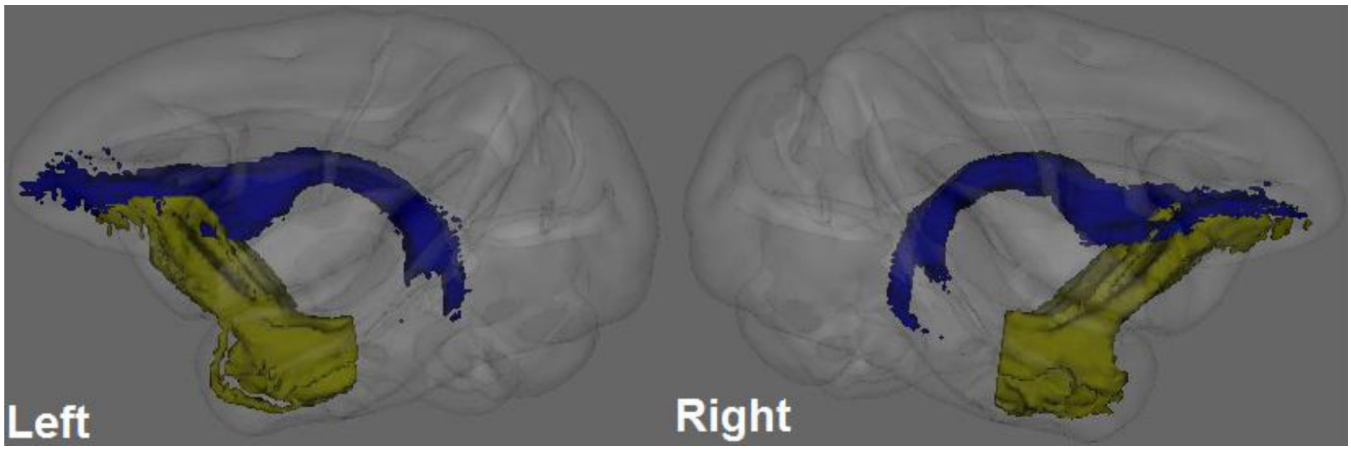

Figure 3.

Fiber tracts connecting fornix and ventromedial prefrontal cortex in the left and right hemispheres passing through fornix (blue color) or temporal stem (yellow color), by probabilistic diffusion tractography. DTI-derived measures were calculated from the correspondent skeletonized map (not shown) within the fiber tracts.

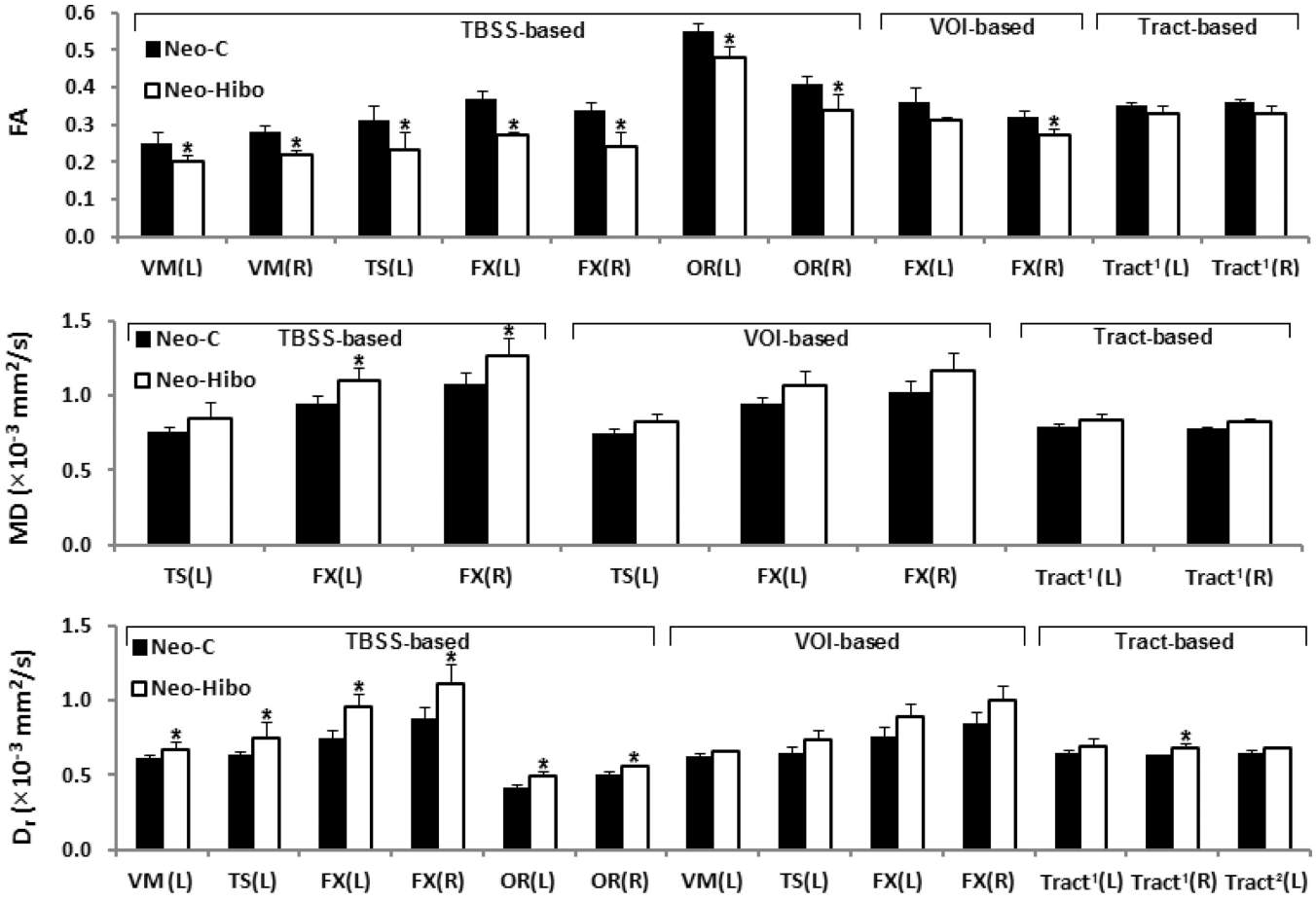

Figure 4.

A graphical representation of DTI-derived measures with significant group difference in Table 1 ($p < 0.05$), and additionally, the star (*) indicating significant group difference with FDR correction. Abbreviation. VM: ventromedial prefrontal cortex; TS: temporal stem; FX: fornix; OR: optic radiations; Tract[1]: tracts connecting hippocampus and VM through FX; Tract[2]: tracts connecting hippocampus and VM through TS; L: left; R: right. VOI: volume of interest.

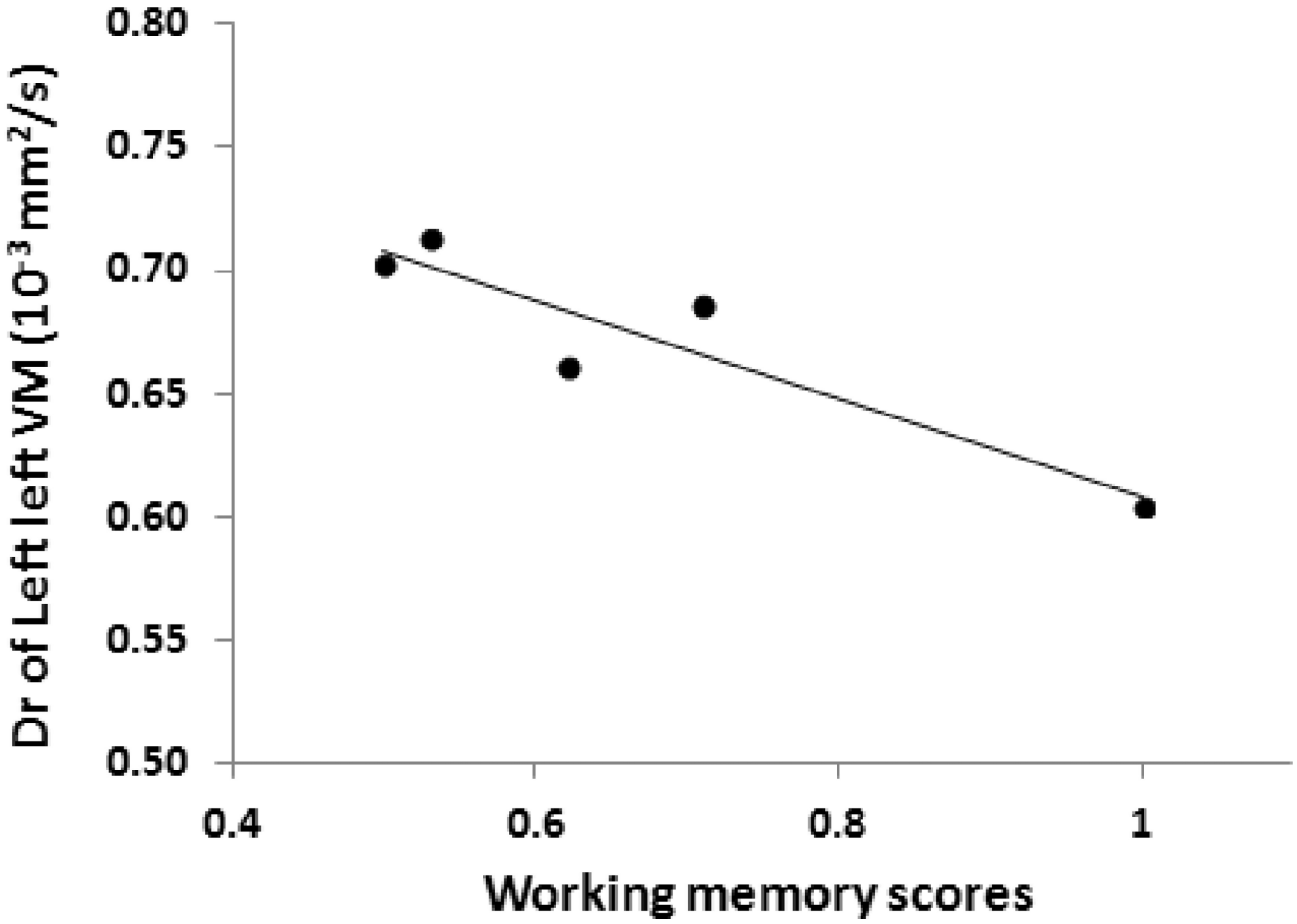

Figure 5.

Radial diffusivity (D_r) values of the left ventromedial prefrontal cortex (VM) in Neo-Hibo group are significantly correlated with working memory scores in serial order task (Pearson's corrections, $p < 0.05$).

Table 1

Group difference in DTI-derived measures based on analysis of TBSS, volume-of-interest and the tracts between hippocampus and VM.

Analysis	FA (Mean±SD)			MD (×10^{-3} mm^2/s) (Mean±SD)			Da (×10^{-3} mm^2/s) (Mean±SD)			Dr (×10^{-3} mm^2/s) (Mean±SD)		
	Neo-C	Neo-Hibo	p	Neo-C	Neo-Hibo	p	Neo-C	Neo-Hibo	p	Neo-C	Neo-Hibo	p
TBSS												
VM L	0.25±0.03	0.20±0.02	**0.013***, *§*	0.72±0.04	0.76±0.07	0.25	0.90±0.05	0.92±0.11	0.74	0.61±0.03	0.67±0.05	**0.024***, *§*
VM R	0.28±0.02	0.22±0.01	**0.003***, *§*	0.77±0.06	0.77±0.06	0.88	1.00±0.09	0.95±0.06	0.36	0.65±0.05	0.69±0.06	0.36
TS L	0.31±0.04	0.23±0.05	**0.037***, *§*	0.76±0.03	0.85±0.10	**0.049***	1.00±0.07	1.05±0.11	0.38	0.64±0.02	0.75±0.11	**0.03***, *§*
FX L	0.37±0.02	0.27±0.01	**<0.001***, *§*	0.94±0.06	1.10±0.09	**0.004***, *§*	1.32±0.08	1.41±0.11	0.16	0.75±0.05	0.95±0.09	**0.001***, *§*
FX R	0.34±0.02	0.24±0.04	**0.001***, *§*	1.08±0.07	1.26±0.13	**0.011***, *§*	1.49±0.07	1.57±0.12	0.18	0.88±0.08	1.11±0.13	**0.004***, *§*
OR L	0.55±0.02	0.48±0.03	**0.003***, *§*	0.67±0.02	0.70±0.06	0.44	1.14±0.02	1.11±0.12	0.63	0.42±0.02	0.49±0.03	**0.042***, *§*
OR R	0.41±0.02	0.34±0.04	**0.002***, *§*	0.69±0.08	0.69±0.03	0.88	1.02±0.11	0.97±0.07	0.39	0.50±0.03	0.56±0.01	**0.03***, *§*
Volume-of-interest												
VM L	0.29±0.03	0.27±0.03	0.38	0.73±0.03	0.77±0.01	0.06	0.97±0.07	0.99±0.04	0.57	0.62±0.03	0.66±0.01	**0.048***
VM R	0.29±0.02	0.28±0.01	0.37	0.76±0.02	0.78±0.02	0.13	0.99±0.04	1.01±0.03	0.29	0.64±0.02	0.66±0.02	0.11
TS L	0.27±0.03	0.25±0.05	0.35	0.75±0.03	0.82±0.06	**0.037***	0.94±0.04	1.00±0.06	0.09	0.65±0.04	0.73±0.07	**0.048***
TS R	0.29±0.02	0.28±0.05	0.69	0.75±0.03	0.76±0.05	0.45	0.97±0.05	0.97±0.03	0.82	0.64±0.02	0.66±0.06	0.37
FX L	0.36±0.04	0.31±0.01	**0.01***	0.94±0.05	1.06±0.10	**0.02***	1.31±0.06	1.39±0.13	1.11	0.76±0.06	0.89±0.09	**0.009***
FX R	0.32±0.02	0.27±0.02	**0.002***, *§*	1.02±0.08	1.17±0.12	**0.03***	1.38±0.08	1.49±0.16	0.12	0.84±0.08	1.00±0.10	**0.01***
OR L	0.51±0.03	0.50±0.04	0.65	0.66±0.03	0.65±0.03	0.77	1.06±0.05	1.04±0.07	0.68	0.46±0.03	0.46±0.03	0.95
OR R	0.48±0.03	0.48±0.03	0.94	0.67±0.04	0.66±0.02	0.58	1.04±0.04	1.03±0.07	0.75	0.49±0.04	0.48±0.01	0.59
CB L	0.40±0.03	0.40±0.01	0.72	0.67±0.02	0.68±0.01	0.48	0.97±0.02	0.98±0.03	0.71	0.52±0.03	0.53±0.01	0.62
CB R	0.42±0.05	0.42±0.03	0.90	0.67±0.02	0.68±0.02	0.42	1.00±0.04	1.01±0.05	0.73	0.51±0.04	0.52±0.02	0.64
CC	0.62±0.03	0.63±0.03	0.80	0.78±0.02	0.79±0.03	0.49	1.41±0.05	1.44±0.04	0.47	0.46±0.03	0.47±0.04	0.76
Tracts between hippocampus and VM												
Tract[1] L	0.35±0.01	0.33±0.02	**0.02***	0.79±0.02	0.83±0.05	**0.048***	1.09±0.01	1.11±0.05	0.33	0.65±0.02	0.69±0.05	**0.045***
Tract[2] L	0.30±0.02	0.29±0.03	0.21	0.78±0.02	0.80±0.02	0.21	1.03±0.02	1.04±0.06	0.83	0.65±0.02	0.68±0.01	**0.035***
Tract[1] R	0.36±0.01	0.33±0.02	**0.037***	0.78±0.01	0.82±0.03	**0.014***	1.08±0.01	1.11±0.04	0.11	0.63±0.01	0.68±0.03	**0.007***, *§*

Analysis	FA (Mean±SD)			MD (×10^{-3} mm^2/s) (Mean±SD)			Da (×10^{-3} mm^2/s) (Mean±SD)			Dr (×10^{-3} mm^2/s) (Mean±SD)		
	Neo-C	**Neo-Hibo**	**p**	**Neo-C**	**Neo-Hibo**	**p**	**Neo-C**	**Neo-Hibo**	**p**	**Neo-C**	**Neo-Hibo**	**p**
Tract^2 R	0.33±0.01	0.32±0.03	0.37	0.76±0.01	0.77±0.01	0.40	1.04±0.02	1.04±0.04	0.98	0.62±0.01	0.64±0.01	0.24

The data were tested with independent t-test with significant level of $p < 0.05$ (* without multiple comparisons correction, § with FDR correction).

Abbreviation. VM: ventromedial prefrontal cortex; TS: temporal stem; FX: fornix; OR: optic radiations; CB: cingulate bundle; CC: corpus callosum; Tract^1: tracts connecting hippocampus and VM through FX; Tract^2: tracts connecting hippocampus and VM through TS; L: left; R: right; SD: standard derivation.

Table 2

Pearson's correlations of memory scores with DTI-derived measures with significant group difference based on analysis of TBSS, volume-of-interest and the tracts between hippocampus (HP) and VM. The memory scores are the ones in serial order working memory and incidental recognition memory task.

Analysis	DTI-derived measures	Correlations of memory scores with diffusivity indices			
		Serial order working memory		Incidental recognition memory	
		r	p	r	p
TBSS					
Left VM	FA/D	0.29/−0.93	0.64/**0.025***	0.29/−0.39	0.72/0.61
Right VM	FA	0.58	0.31	−0.43	0.57
Left TS	FA/MD/D_r	0.21/0.37/0.16	0.73/0.54/0.80	0.78/−0.04/−0.30	0.22/0.96/0.71
Left FX	FA/MD/ D_r	−0.10/0.02/−0.01	0.88/0.98/0.99	0.39/0.42/0.33	0.62/0.58/0.67
Right FX	FA/MD/ D_r	0.24/−0.04/−0.11	0.70/0.95/0.86	0.38/0.27/0.14	0.62/0.73/0.86
Left OR	FA/ D_r	0.16/0.20	0.80/0.74	−0.62/0.92	0.38/0.08
Right OR	FA/ D_r	0.41/0.42	0.49/0.49	0.06/0.64	0.94/0.36
Volume-of-interest					
Left VM	D_r	−0.33	0.58	0.21	0.80
Left TS	MD/ D_r	0.11/−0.05	0.86/0.94	0.40/−0.49	0.60/0.51
Left FX	FA/MD/ D_r	−0.10/0.02/−0.01	0.88/0.98/0.99	0.64/0.16/0.11	0.36/0.84/0.89
Right FX	FA/MD/ D_r	0.24/−0.04/−0.11	0.70/0.95/0.86	0.64/0.05/−0.04	0.36/0.95/0.96
Tracts between HP and VM					
Left Tract[1]	FA/MD/ D_r	0.42/−0.22/−0.22	0.48/0.72/0.72	0.31/−0.12/−0.14	0.69/0.88/0.87
Right Tract[1]	FA/MD/ D_r	0.30/0.21/0.09	0.62/0.73/0.89	0.35/−0.17/−0.30	0.65/0.83/0.71
Left Tract[2]	D_r	0.04	0.95	0.62	0.38

In consideration of the small sample size, a significant level of *$p < 0.05$ without multiple comparisons correction was adopted in this study.

Abbreviation. VM: ventromedial prefrontal cortex; TS: temporal stem; FX: fornix; OR: optic radiations; Tract1: tracts from hippocampus to VM through FX; Tract2: tracts from hippocampus to VM through TS.